Water Air Soil Pollut (2025) 236:998
https://doi.org/10.1007/s11270-025-08671-y

# Thymol–Menthol-Based Deep Eutectic Solvents for Efficient Rhodamine B Remediation: Molecular Interactions, Economic Feasibility, and Environmental Assessment

**Ghee Kang Zheng · Siti Khalijah Mahmad Rozi · Qian Yee Ang · Rafizah Rahamathullah · Saleha Shamsudin · Fairuz Liyana Mohd Rasdi · Mohd Faisal Taha · Nidal M. Hussein · Faisal Aburub**

Received: 20 December 2024 / Accepted: 24 September 2025 / Published online: 7 October 2025
© The Author(s) 2025

**Abstract** Deep eutectic solvents (DESs), derived from natural and biodegradable resources, are promising alternatives to organic and ionic solvents. In this study, Thymol-Menthol-based deep eutectic solvents (T:M) were prepared, with Thymol serving as the hydrogen bond donor (HBD) and Menthol as the hydrogen bond acceptor (HBA) in various molar ratios (1:1, 1:2, 1:3, 1:4, 2:1, 3:1, and 4:1). Fourier Transform Infrared Spectroscopy (FTIR) confirmed the formation of intermolecular interactions, such as hydrogen bonds, between the precursors. $^{1}H$ and $^{13}C$ Nuclear Magnetic Resonance (NMR) analyses validated the molecular structure of the solvents, while Thermogravimetric Analysis (TGA) demonstrated their thermal stability, with decomposition occurring at temperatures above 150 °C. For Rhodamine B (RB) remediation, the proposed DESs exhibited a shorter extraction time (10 min) and minimal solvent volume requirement (400 µL) compared to traditional organic solvents. COSMO-RS (Conductor-like Screening Model for Real Solvents) simulations revealed that the DESs possess a strong affinity for non-polar, hydrogen-bond-donating, and hydrogen-bond-accepting molecules, confirming their exceptional extraction efficiency for RB, primarily driven by hydrophobic interactions and hydrogen bonding. The studied DESs achieved high removal efficiencies (70–98%) for multiple textile dyes, including Methylene Blue (MB), Crystal Violet (CV), and Safranin (SR). Notably, phytotoxicity assessments indicated no adverse effects on Pisum

**Supplementary Information** The online version contains supplementary material available at https://doi.org/10.1007/s11270-025-08671-y.

G. K. Zheng · S. K. M. Rozi (✉) · Q. Y. Ang · R. Rahamathullah · S. Shamsudin
Faculty of Chemical Engineering & Technology, Universiti Malaysia Perlis, Kompleks Pusat Pengajian Jejawi, 02600 Arau, Perlis, Malaysia
e-mail: khalijahrozi@unimap.edu.my

S. K. M. Rozi
Centre of Excellence for Biomass Utilization, Universiti Malaysia Perlis, 02600 Arau, Perlis, Malaysia

F. L. M. Rasdi · M. F. Taha
Fundamental and Applied Sciences Department, Universiti Teknologi PETRONAS, Seri Iskandar, 32610 Perak, Malaysia

F. L. M. Rasdi · M. F. Taha
Centre of Research in Ionic Liquids, Universiti Teknologi PETRONAS, Seri Iskandar, 32610 Perak, Malaysia

N. M. Hussein
Department of Civil Engineering, Faculty of Engineering, University of Petra, Amman, Jordan

F. Aburub
Faculty of Administrative & Financial Sciences, University of Petra, Amman, Jordan

sativum (pea) seed germination at low concentrations. The EcoScale score tool also verified that the solvent synthesis process is both environmentally benign and worker-safe. These findings underscore the potential of studied DESs as sustainable, high-performance extractants for the remediation of dye-contaminated wastewater.

**Keywords** Conductor like screening model for real solvents · Deep eutectic solvents (DESs) · Dye · EcoSscale · Menthol · Phytotoxicity · Thymol

## 1 Introduction

Water pollution has become one of our most pressing environmental challenges, demanding immediate and coordinated action to mitigate its impacts and safeguard the cleanliness and safety of water resources for daily use (Tiwari et al., 2022). The widespread use of synthetic dyes, mainly Rhodamine B (RB), across industries such as cosmetics, food, textiles, paints, printing, and plastics manufacturing has resulted in the discharge of substantial amounts of coloured, toxic effluents. These pollutants often contaminate surface water and groundwater, posing significant environmental and public health risks (Behbahani et al., 2021). Liquid–liquid extraction (LLE) is considered one of the effective techniques for dye remediation from wastewater treatment with various advantages, such as simplicity, scalability, and high recovery rates (Khatibi et al., 2022). However, the extractants commonly used in liquid–liquid extraction (LLE) are typically organic solvents such as ethanol, hexane, and toluene. These solvents are often required in long extraction times and substantial volumes, and are highly volatile, raising significant concerns about environmental pollution and human health (Brijmohan et al., 2021). Among these, ionic liquids (ILs) have emerged as next-generation replacements for conventional organic solvents in various applications (Alqahtani, 2024; Chen & Mu, 2021; Chen et al., 2023a). One of the green solvents, ionic liquid (IL), originates from molten organic salts consisting of free-moving cations and anions in a liquid state at ambient temperatures (Jin et al., 2021; Rahman et al., 2022; Zhao et al., 2021). ILs are recognised as green solvents due to their unique properties, negligible vapour pressure (Fabre & Murshed, 2021; Zhang et al., 2023), tunable viscosity (Bouarab et al., 2021), and high thermal stability (Kianfar & Mafi, 2021; Singh & Savoy, 2020) encourage the replacement of organic solvents with ILs. The costly (Wang et al., 2021; Zhu et al., 2021), challenging synthesis and purification (Singh & Savoy, 2020), enabling researchers to explore other eco-friendly solvents.

Deep eutectic solvents (DESs) have recently become the new trend in green solvents. DESs originate from binary or tertiary (Hansen et al., 2020; Velez & Acevedo, 2022) mixtures of compounds, with both hydrogen bond acceptor (HBA) and hydrogen bond donor (HBD) (Mero et al., 2023) to form a new eutectic compound. These solvents possess unique combinations of physicochemical properties with high thermal stability (Cotroneo-Figueroa et al., 2022; Marchel et al., 2022), negligible vapour pressure (Peng & Minceva, 2024), low cost and simple preparation processes, making them an excellent alternative source of green solvents (Chabib et al., 2022; Ijardar et al., 2022; Martínez et al., 2022; Sekharan et al., 2022). DESs are widely used in various applications, including biodiesel production (Malolan et al., 2021), nanomaterial and polymer synthesis (Nahar & Thickett, 2021; Nam et al., 2023), biochemistry, and biocatalysis (Panić et al., 2021). For environmental applications, DESs have been used for the treatment of lead from mangrove soil (Rashid et al., 2022), crude oil (Duan et al., 2021), phenolic compounds (Zheng et al., 2022), Cadmium (Lamarca et al., 2024) dyes, and nanoplastics (Chen et al., 2023b). Despite extensive research underscoring the effectiveness of deep eutectic solvents (DESs) as superior remediation agents, a critical gap remains in the comprehensive evaluation of Thymol-Menthol-based deep eutectic solvents (T:M) across various molar ratios and their potential as potent extractants for dye remediation, particularly for RB. Furthermore, no studies have systematically compared these DESs with conventional solvents for liquid–liquid extraction of dyes, particularly in extraction time, solvent volume, and EcoScale analysis. Additionally, data on the phytotoxicity of these DESs remain scarce.

The primary goal of this study is to develop cost-effective Thymol-Menthol-based deep eutectic solvents (T:M) as extractants for RB. Thymol and Menthol, natural monoterpenoids, serve as precursors for preparing T:M. Thymol, also known as

2-isopropyl-5-methylphenol (IPMP), has the molecular formula $C_{10}H_{14}O$ and is a phenolic monoterpenoid derived from p-Cymene (Baginska et al., 2023; Krause et al., 2021). It has an aromatic odour and naturally occurs in thyme essential oil (Yu et al., 2021). Menthol, a monoterpenoid alcohol (Oshima & Ito, 2021; Tian et al., 2023) with the formula $C_{10}H_{20}O$, is known for its refreshing flavour and can be sourced naturally or synthesised (Oshima & Ito, 2021). Thymol and Menthol were selected due to their low cost, natural origin, and biodegradable nature (Jiang et al., 2025), in alignment with the core principles of green chemistry. Moreover, they possess multiple functional groups such as aromatic rings, hydroxyl groups, and alkyl chains that can interact with organic dyes via π-π stacking, hydrogen bonding, and hydrophobic interactions. These mechanisms enhance the binding efficiency between the T:M and dyes, making it a highly promising candidate for textile wastewater treatment. The physical and chemical properties of the prepared T:M were thoroughly characterised, and their effectiveness was tested against model dye pollutants, primarily RB. Quantum chemical calculations using COSMO-RS were employed to predict molecular interactions between T:M and RB. Furthermore, comparative analysis of dye removal performance between T:M and conventional organic solvents, and EcoScale assessment were conducted to evaluate chemical processes at the laboratory scale based on factors such as cost-effectiveness, high yield, and minimal risk to the operator and the environment. Additionally, the influence of pH, the removal efficiency of various dyes (Methylene Blue (MB), Crystal Violet (CV), and Safranin (SR)), and phytotoxicity were examined to demonstrate the effectiveness of the proposed DES. This study aims to deepen the understanding of the fundamental properties and performance of the developed materials, ultimately contributing to developing more efficient and sustainable tools for environmental remediation.

## 2 Materials and Methods

### 2.1 Materials

Thymol (> 99% purity) and Menthol (> 98% purity) were purchased from Sigma-Aldrich (Germany). The chemicals were used without any further purification. Ultrapure water was obtained using a Mili-Q water purification system. Stock solutions of Rhodamine B (RB), Methylene Blue (MB), Crystal Violet (CV), and Safranin (SR), were prepared in ultrapure water with a concentration of 100 ppm and kept in a refrigerator at 4 ℃.

### 2.2 Preparation of T:M

In this study, T:M was synthesised using a heating method described by Nguyen et al. (Nguyen et al., 2021). In brief, Thymol and Menthol were heated to 80 °C with continuous stirring, using molar ratios of 1:1, 1:2, 1:3, 1:4, 2:1, 3:1, and 4:1 until a clear liquid formed. Then, the obtained liquid was left aside to cool to room temperature.

### 2.3 Characterizations of T:M

$^{1}$H-NMR and $^{13}$C-NMR of synthesised DESs were recorded on a 400 MHz NMR spectrophotometer (model: Bruker Advance, USA) using TMS as an internal standard to confirm the molecular structure of DESs. The samples were prepared at about 30 mg in NMR tubes and dissolved in 0.5 mL of deuterated chloroform, $CDCl_3$. Fourier Transforms Infrared Spectroscopy (FTIR) analysis using Spectrum 400 Perkin Elmer (Waltham, MA, USA) in the spectral range of $4000 - 400\ cm^{-1}$ and a resolution of $\pm 4\ cm^{-1}$ examined the functional groups and hydrogen bond formation between Thymol and Menthol, confirming the formation of a eutectic mixture. In addition, Thermogravimetric Analysis (TGA) was performed to measure the mass loss from 30 °C to 700 °C, along with Differential Thermal Analysis (DTA) to assess the heat input and phase transition of T:M using a PerkinElmer thermal analyser. UV–Vis spectrophotometer analysis (UV-1080, Shimadzu, Japan) was used to measure the absorbance of residual studied dyes, RB (λ = 554 nm), MB (λ = 664 nm), CV (λ = 590 nm), and SR (λ = 520 nm) in water after the removal process.

### 2.4 COSMO-RS Simulation Study

The thermodynamic properties of the proposed DES and RB were analysed using the COSMO-RS method. The computational sequence began with optimising

the RB structure. Since RB's structure is available in PubChem, the SMILES format was imported into TMoleX (TURBOMOLE, version 4.4.1) to build the 3-D model of the molecule. This structure was then optimised using TMoleX, and the file was saved in the COSMO format. The def-TZVP basis set and B3-LYP functional were employed for density functional theory (DFT) calculations. The optimised geometry of RB was then sent to the COSMO database. Thymol and Menthol, available in the COSMOthermX database, were directly utilised. Using COSMOthermX (version 19.0.4) with BP-TZVP parameterisation, the prediction of all studied thermodynamic properties was conducted, and this data was used to express the solvent–solute chemical potentials of the DES and RB.

In the COSMO-RS prediction process, the solute molecules are first surrounded by a virtual conductor, established using the continuum solvation model. In this model, the solvent is represented as a continuous medium with a uniform dielectric constant, rather than as discrete molecules. The virtual conductor serves as an idealised concept where the solute is placed within a hypothetical conductor. The screening charge density distribution (σ-profile) is then calculated for the solute using quantum chemical methods. The σ-profile characterises how the virtual conductor screens the solute's electric field, resulting in a specific charge distribution on the solute's surface.

This three-dimensional surface charge density distribution of the molecule can be converted into a histogram plot called a σ-profile, $P(\sigma)$ based on Eq. (1) (Khan et al., 2023).

$$\mathrm{P}(\sigma) = \sum\nolimits_{\mathrm{i}} \mathrm{x_i P^{x^i}}(\sigma) \tag{1}$$

where $\S_i$ denotes the molar fraction of the i. segment, cap P to the script x to the i. end superscript referred to as the σ-profile of the I segment, and I represents a specific component in the mixture. The σ-profile describes the polarity of the molecules. In contrast, the electrostatic potential derived from the σ-profile, known as the σ-potential, describes the interaction behaviour and affinity between molecules in the system. The σ-potential, $\mu$ (σ) of molecules is calculated using Eq. (2) based on the calculated σ-profile using the Klamt equation:

$$\mu(\sigma) = -TRIn\left(\int d\sigma' P(\sigma).e^{\left(\left(-1/2\right)_a{}'^{(\sigma+\sigma')^2} - ((\mu'(\sigma'))/RT)\right)}\right) \tag{2}$$

where α' refers to a general interaction fitting parameter to describe the energy of the geometrically optimised structure of the molecule, and the μ(σ) denotes the chemical potential.

From the σ-profile and σ-potential, various interaction energies and hydrogen bonding properties can be predicted, including misfit interaction energy ($E_{MF}$), van der Waals interaction energy ($E_{vdW}$), hydrogen bond acceptor moment ($M_{HBA}$), and hydrogen bond energy ($E_{HB}$). Mathematically, the energies are described using the following Eqs. (3)– (5):

$$E_{MF}(\sigma,\sigma') = {}_{eff.}\left(a'/2\right)\left(\sigma+\sigma'\right)^2 \tag{3}$$

$$E_{HB} = a_{eff.}\, c_{HB} min\left(0, \sigma\sigma' + {\sigma_{HB}}^2\right) \tag{4}$$

$$E_{vdW} = a_{eff.}\left(\tau_{vdW} + \tau_{vdW}\prime\right) \tag{5}$$

where the $\alpha_{eff}$ represents the effective contact area between two surface segments, $c_{HB}$ is denoted as the hydrogen bonding interaction strength coefficient, $\sigma_{HB}$ is the charge density threshold for hydrogen bonding. In contrast, the general fitting for van der Waals interaction is represented by $\tau_{vdW} + \tau_{vdW}\prime$.

## 2.5 Dye Removal

The removal process of RB dye was adapted from a modified version of Chen et al. (Chen et al., 2024). Each 400 μL of T:M at the studied molar ratios was briefly added to a 6 mL aliquot containing 10 ppm of RB. After shaking the sample for 10 min using a shaker, it is centrifuged at 4000 rpm for 5 min, separating the solution into two phases: T:M phase, containing extracted RB dye, and a clear aqueous phase. The RB removal efficiency was then analysed using a UV–Vis Spectrophotometer and calculated using Eq. (6).

$$\textit{Extraction efficiency}\ (\%) = \frac{C_i - C_0}{C_i} \times 100\% \tag{6}$$

where $C_i$ and $C_0$ represent the dye's concentration before and after removal, respectively, several parameters, such as the volume of T:M, contact time, and the solution's pH, that influence the RB dye removal efficiency were studied and optimised. The removal of additional dyes, including MB, CV and SR, was also evaluated under the same optimised conditions. Additionally, the dye removal efficiencies of conventional solvents like toluene and benzene were examined in this study.

### 2.6 Evaluation of Greenness

**EcoScale Analysis** The EcoScale method was used to evaluate chemical conditions on a laboratory scale, including using inexpensive compounds, high yield, and minimal risk for the operator and the environment (Mejías et al., 2025). The ideal green analysis in the method was assigned 100 points, which were penalty points (PPs) according to the yield, price of raw materials, safety, temperature/time and workup and purification. Starting with the ideal analysis method of 100 points, PPs reduce the score for the actual method. Projects scoring more than 75 points represent excellent green analyses, and those with acceptable green analyses score more than 50 points. In the dye removal extraction process, penalty points were assigned based on factors such as the types of chemicals or reagents used, energy consumption of equipment, occupational hazards, and waste production. Beginning with a perfect 100, the actual method's score is reduced by the penalty points. The greener the process, the closer it remains to the ideal score of 100 (Freire et al., 2025).

**Phytotoxicity** Phytotoxicity of the DES was assessed using a seed germination assay with *Pisum sativum* (pea) seeds, based on modified protocols from previous studies (Kang Zheng et al., 2025; Yap & Gan, 2024). Briefly, ten seeds were placed in individual petri dishes lined with filter paper and a thin layer of cotton wool, then moistened with 5 mL of DES solutions at concentrations of 0.001%, 0.01%, 0.1%, and 1% (w/v). A control group was maintained using 5 mL of freshwater. The assay was conducted under controlled temperature, air circulation, and darkness conditions. After seven days of incubation, the germination percentage (% Germination) was calculated using Eq. (7):

$$\%\ Germination = \frac{Number\ of\ seeds\ germinated}{Total\ number\ of\ seeds} \times 100\% \quad (7)$$

## 3 Results and Discussion

### 3.1 Visual Observations of T:M

Table 1 presents the appearance of the prepared Thymol-Menthol-based deep eutectic solvents (T:M) at molar ratios of 1:1, 1:2, 1:3, 1:4, 2:1, 3:1, and 4:1. The results show that all prepared T:M samples were clear liquids after the heating process, except the 3:1 and 4:1 molar ratios. Moreover, the clear liquids of T:M remained viscous and transparent over time, indicating the stability of the synthesised DESs. This observation is consistent with findings by Uğan et al. (Uğan et al., 2024), who prepared choline chloride:phenol-based DESs at 1:1, 1:2, and 1:3 molar ratios.

### 3.2 Characterizations of T:M

FTIR was conducted to investigate the essential functional groups and determine the formation of hydrogen bonds between T:M. Figure S1 illustrates the FTIR spectra with band characteristics of functional groups of five various molar ratios of T:M, Thymol, and Menthol. Menthol presented absorption peaks at 3208 $cm^{-1}$, 2921 $cm^{-1}$, and 2853 $cm^{-1}$, corresponding to the O–H band, asymmetric and symmetric $CH_2$ stretching, respectively. The 1395–1334 $cm^{-1}$ peaks correspond to O–H in-plane bending vibration, while the peak at 1289 $cm^{-1}$ is attributed to the isopropyl group. Moreover, the peak signal at 1291 $cm^{-1}$ is attributed to C-O stretching, and the peak at 806 $cm^{-1}$ corresponds to the out-of-plane aromatic C-H (Zheng et al., 2025). Thymol's absorption peaks at 3198 $cm^{-1}$, 1340 $cm^{-1}$, 2991 $cm^{-1}$, and 2893 $cm^{-1}$ are attributed to O–H stretching, O–H bending, and asymmetric and symmetric $CH_2$ stretching, respectively. Furthermore, the peaks in the range 1467–1419 $cm^{-1}$ are due to the C=C stretching of the benzene ring of Thymol (Sharifi et al., 2025).

All peaks that appeared for Thymol and Menthol were observed in the spectra of all prepared T:M at different ratios. Additionally, the OH stretching band of the studied T:M was observed to shift to a higher

wavelength (as shown in Figure S1), which signifies the formation of a eutectic mixture. This outcome strongly suggests the existence of hydrogen bonding between individual constituents (Thymol and Menthol) in the prepared DESs. Similar results were reported by Qi et al. (2025); Zhang et al., 2022). Functional groups analysis proved that the fabricated T:M, consisting of hydroxyl groups, aliphatic compounds, and aromatic moieties, could be responsible for hydrogen bonding and hydrophobic and pi-pi interactions with water pollutants in environments such as organic dyes.

Further analyses using $^{1}$H NMR and $^{13}$C NMR spectroscopy were performed to determine the types of protons and carbon in the synthesised T:M and the spectra presented in Figures S2 and S3, respectively. In the $^{1}$H NMR spectrum, T:M 1:1 shows the chemical shift values around $\delta = 1.4$ ppm and 2.4 ppm due to methyl (**peaks no. 1, 2**) and methylene (**peaks no. 5, 6, 7**) protons of Thymol, respectively (Mydeen et al., 2022). The peaks at $\delta = 4.7$ ppm corresponded to hydroxyl groups (**peaks no. 4, 11**) of Thymol and Menthol (Sereshti et al., 2021; Zhao et al., 2025). The $\delta = 0.9$ ppm attributed to the methyl group of Menthol with **peaks** of **1 and 3,** respectively. The range of $\delta = 1.0$–2.4 ppm and 3.3 ppm (**peaks no. 4, 5, 6, 7, 8, and 9**) indicates the methylene groups of Menthol (Zhao et al., 2025). In the $^{13}$C NMR, the peak with $\delta = 16$–24 ppm corresponds to methyl (**peaks no**. **8, 9, 10**: **1, 3**) and methylene carbons (**peaks no. 7**, **3**) for both Thymol and Menthol, respectively (Sereshti et al., 2021; Zheng et al., 2025). The signals for benzyl groups of Thymol (**peaks no. 1, 2, 3, 4, 5, 6**) constituents are observed at $\delta = 116$–153 ppm. Spectra of T:M 1:2 to T:M 2:1 also presented comparable peaks similar to T:M 1:1, confirming the structure of the synthesised T:M in the present study.

TG thermograms combined with DTA of the five molar ratios of T:M, T:M 1:1 to T:M 2:1 are presented in Figure S4. The derivative peaks presented by DTA indicate the information on the mass loss steps and the temperature of the maximum rate of change in weight loss (El-Sayed et al., 2024). The onset decomposition temperature indicates the initial decomposition temperature and was used to study the maximum temperature for T:M, which remains in the liquid state without decomposition (Rahman et al., 2025). As seen in the figure, the decomposition temperature for all T:M started around 120 ℃ and was lower than their constituents, Thymol (201℃) and Menthol (181℃), respectively. For the DTA thermogram, major derivative peaks range from 170 ℃ to 185 ℃, revealing a one mass loss step caused by decomposing precursors of the studied DESs in a single step. A similar finding was reported by Trivedi (Ahmed et al., 2025; Hussin et al., 2020). These results proved that the as-prepared DESs are non-volatile solvents as they showed good thermal stability at room temperature and could be employed as an ideal extractant for the remediation of organic pollutants from environmental samples.

## 3.3 COSMO-RS Study

### *3.3.1 σ-Profile and σ-Potential of Precursors of T:M*

The σ-profile denotes the polar and non-polar nature of the Thymol and Menthol in this study, and the results are shown in Fig. 1(A). The histogram of probability distribution curves can be divided into three primary regions: the hydrogen bond donor (HBD) region ($\sigma < -0.0086$ e/Å$^2$), hydrogen bond acceptor (HBA) region ($\sigma > 0.0086$ e/Å$^2$), and the non-polar region ($-0.0086$ e/Å$^2 < \sigma < 0.0086$ e/Å$^2$) (Hussin et al., 2021). Positive surface charges appear in the negative σ region, while negative surface charges appear in the positive σ region, with the middle segment corresponding to neutral regions (Khan et al., 2021). As seen in the result, the precursors of the present DESs, Thymol and Menthol, exhibit distinct and strong peaks in the neutral regions, specifically at $\sigma = -0.002$ e/Å$^2$ and $-0.003$ e/Å$^2$, respectively. In addition, it was revealed that Thymol and Menthol possess both HBD and HBA properties as they are observed in the negative σ region ($-0.0021$ e/Å$^2 < \sigma < -0.013$ e/Å$^2$) and positive σ region at 0.011 e/Å$^2 < \sigma < 0.010$ e/Å$^2$. Since Thymol and Menthol exhibit both HBD and HBA properties, they tend to form hydrogen bonds with each other, contributing to the stability of the prepared DESs, T:M.

As seen from the σ-potential distribution (Fig. 1 (B)), Thymol has the highest affinity for interacting with hydrogen bond acceptors (Quaid & Reza, 2023). At the same time, Menthol shows the most significant capability for interacting with hydrogen bond donors. This suggests that the interaction between the components of the T:M occurs through hydrogen bonding, where Thymol acts as the hydrogen bond donor, and Menthol acts as the hydrogen bond acceptor.

**Table 1** Visual observations of the different mixtures of T:M

| DESs | Observation | | Appearance |
|---|---|---|---|
| | After heating | After 1 month | |
| T:M 1:1 | Transparent liquid | Transparent liquid |  |
| T:M 1:2 | Transparent liquid | Transparent liquid |  |
| T:M 1:3 | Transparent liquid | Transparent liquid |  |
| T:M 1:4 | Transparent liquid | Transparent liquid |  |
| T:M 2:1 | Transparent liquid | Transparent liquid |  |
| T:M 3:1 | Solid | Cloudy solution |  |
| T:M 4:1 | Solid | Cloudy solution |  |

### 3.3.2 σ-Profile and σ-Potential of T:M at Various Molar Ratios

The σ-profile of T:M in Fig. 2(A) was calculated based on the mole fraction of each component of the studied DESs. All prepared T:M is predominantly non-polar, polar hydrogen-bond donating, and polar hydrogen-bond accepting, similar to its constituents (Thymol and Menthol). It could be expected that the studied analyte, RB will be more soluble in the less polar T:M than in the more polar water solvent, thus enhancing the affinity of this analyte during the removal process. A similar trend is observed for σ-potential plots of T:M (Fig. 2 (B)): they are parabolic in the nonpolar region, indicating their nonpolar. All studied T:M demonstrate a favourable nonpolar interaction with hydrophobic compounds. In addition, T:M also shows a parabolic curve in the hydrogen donor and acceptor sections with a negative value. This implies that the as-prepared T:M has a strong affinity towards hydrogen-bond donating and the hydrogen bond accepting molecules, suggesting a desirable hydrogen bond interaction with the hydrogen bond acceptor and the hydrogen bond donor of the studied extractants. The σ-potential plots for all synthesised solvents display a comparable trend. Among σ-potential plots of all T:M, T:M 2:1 exhibits the highest attraction to interact with hydrogen bond acceptors, followed by T:M 1:1, T:M 1:2, T:M 1:3 and T:M 1:4, This suggests that T:M 2:1 has the strongest affinity for the protons in dye molecules during the removal process.

### 3.3.3 Molecular Interactions of T:M Using Interaction Energies

Based on their molar ratios, the molecular interactions between Thymol and Menthol in the prepared DESs were predicted using COSMO-RS, with the data presented in Fig. 3. The results indicate that van der Waals energy ($E_{vdW}$) is the predominant interaction between Thymol and Menthol in all the prepared DESs, followed by hydrogen bonding ($E_{HB}$) and Misfit's Electrostatic Energy ($E_{MF}$). This observation can be attributed to the σ-profile of the precursors, which showed prominent peaks in the nonpolar region, suggesting that van der Waals forces primarily drive their interaction. Moreover, the hydrogen bonding ($E_{HB}$) of the developed DESs can be described by the interaction between the oxygen and proton of both precursors during the synthesis of the DESs. These interactions may indicate the stability of the formulated DESs, suggesting a stable adsorption and removal process when using these extractants.

## 3.4 Application: T:M as an Extraction Solvent for the Removal of Toxic Rhodamine B dye

Rhodamine B (RB) dye is commonly utilised as a synthetic dye in the textile industries (Al-Buriahi

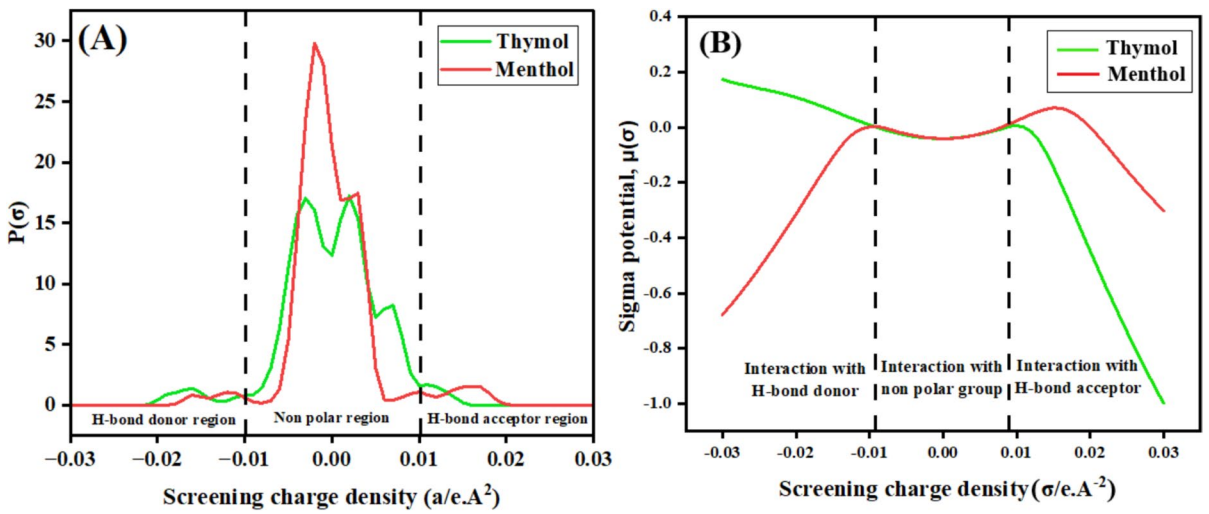



**Fig. 1** Predicted **A** σ profile and **B** σ potential distributions of Thymol and Menthol using the COSMO-RS model

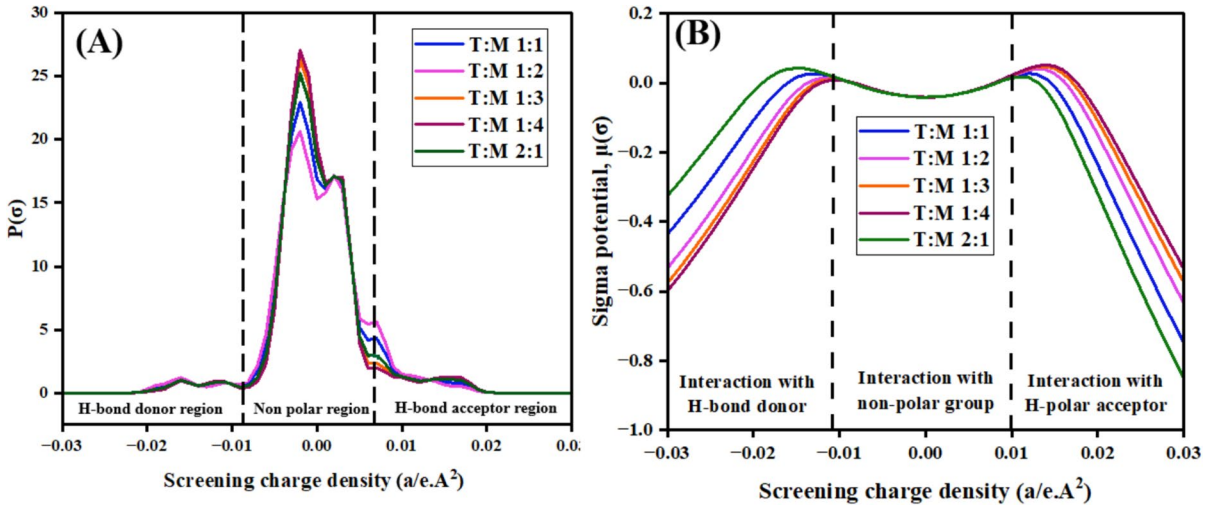



**Fig. 2** Predicted **A** σ profile and **B** σ potential distributions of various molar ratios of T:M using the COSMO-RS model

et al., 2022), such as paper (Thakur & Kaur, 2017), paint, etc. (Saigl, 2021), by manufacturers due to its thermal and light stability and biodegradability (Saigl, 2021). However, intensive RB dye causes potential carcinogenic and mutagenic effects on humans and animals upon prolonged contact, causing skin and respiratory inflammation (Al-Gheethi et al., 2022; Amalina et al., 2022). Therefore, it is imperative to remove RB dye from wastewater effluent before discharging it into water sources to safeguard the environment.

Hence, the performance of prepared T:M was examined to remove RB using a liquid–liquid extraction procedure, and their removal performance was analysed using a UV–Vis spectrophotometer. The results show that the UV absorbance of RB significantly decreased after treatment with T:M in all studied molar ratios, compared to the initial concentration. This indicates that the T:M in all tested ratios are effective extractants for RB remediation, achieving removal efficiencies between 92 and 99% in this study (Fig. 4(A) and (B)). This phenomenon may be attributed to the strong electrostatic, hydrophobic, and π-π interactions between the prepared T:M and RB pollutant. To further investigate these interactions, the potential interactions of RB with the studied T:M were analysed using COSMO-RS.

### *3.4.1 Molecular Interactions of RB and T:M*

Σ-profile of RB demonstrates that it is mostly nonpolar, but it also has a small region with σ = 0.012 e/Å2 at the H-bond acceptor region, indicating hydrogen-bond accepting ability. The prominent peaks in the nonpolar region are attributed to the methyl and phenyl groups of the RB structure, which can interact with the aromatic ring and methyl group of the DESs through hydrophobic interactions. Furthermore, its hydrogen bond-accepting capability is linked to the polar oxygen atoms in the carboxylic group. These oxygen atoms can interact with protons of the T:M extractants to form hydrogen bonds. Both hydrogen bonding and hydrophobic interactions between the RB molecule and T:M compounds are evident. based on Fig. 5(A). This result is consistent with the σ-surface of RB (Fig. 5(B), which revealed that RB primarily comprises neutral regions, followed by electropositive regions (hydrogen atoms), partially electronegative sites (C = C), and electronegative regions (oxygen atoms). This finding suggests that RB can form hydrophobic and hydrogen bonds with the extractant during removal. A similar observation was reported by Adeyemi et al. (2020), indicating that COSMO-RS predictions for removing chlorophenol suggested potential interactions are mainly from hydrophobic interactions and hydrogen bonding.

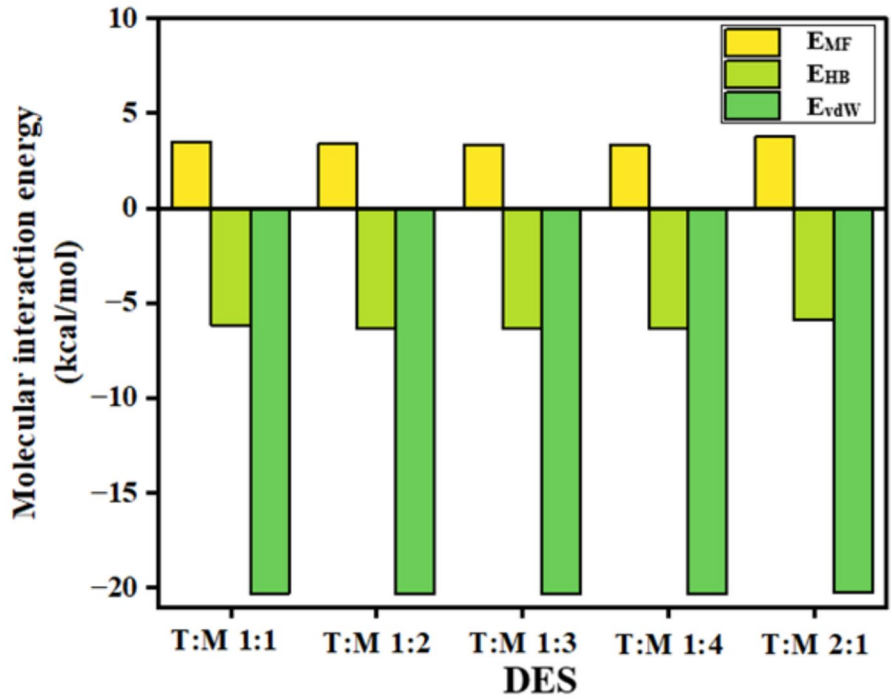



**Fig. 3** Molecular interactions energy of various molar ratios of T:M

The σ-potential curves of RB (Fig. 5(C)) indicate that it can interact with nonpolar compounds. Additionally, RB displays a parabolic curve with a negative value in the hydrogen donor and acceptor regions. This suggests that RB has strong intermolecular interactions with hydrogen-bond-donating and hydrogen-bond-accepting molecules. It can be inferred that hydrogen bonding and hydrophobic interactions are the principal mechanisms driving the removal of RB. Moreover, the interaction energy (the electrostatic misfit energy, $E_{MF}$, the hydrogen bonding energy, $E_{HB}$ and the Van der Waals energy, $E_{vdW}$) between RB and all studied DESs was also assessed using COSMO-RS. Figure 5(D) illustrates that the interaction energies

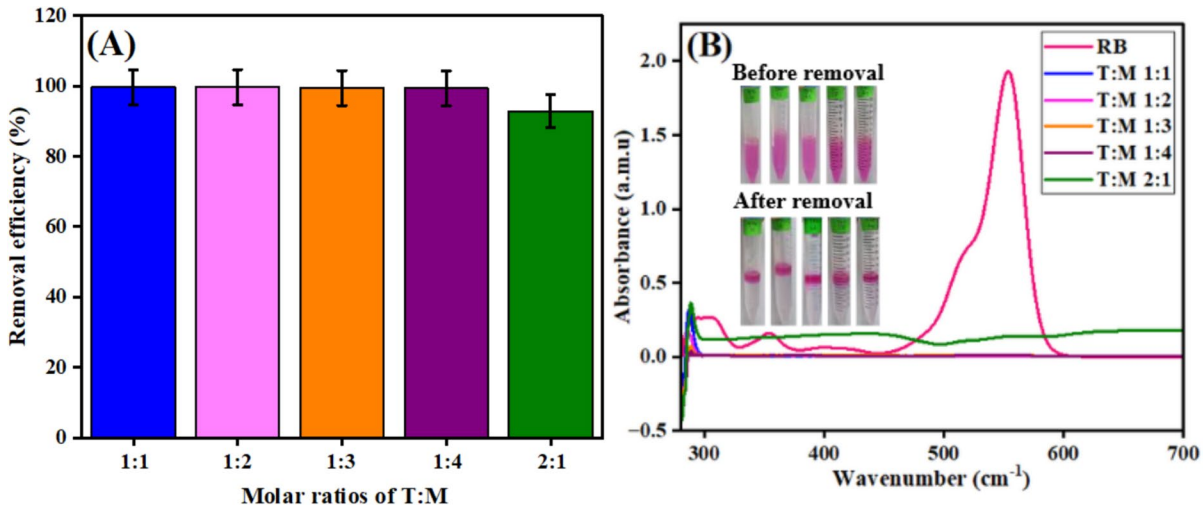



**Fig. 4** **A** The dye removal efficiency of various molar ratios of T:M, **B** UV–Vis absorbance of the initial concentration of RB and after treatment with various molar ratios of T:M

between the prepared extracting solvents and the RB pollutant are consistent throughout the removal process, corroborating the experimental removal results obtained for all T:M ratios. Furthermore, the interaction energy results indicate that $E_{vdW}$ is the predominant interaction in RB adsorption, with $E_{HB}$ and $E_{MF}$ as secondary contributors. The findings from the σ-profile and σ-potential analyses in the COSMO-RS models are in robust alignment.

### 3.5 Economic Feasibility and Environmental Impact of T:M

The cost of preparing deep eutectic solvents is primarily driven by the price of raw materials and synthesis parameters, including synthesis time, the volume of the synthesised solvent, and equipment power. These factors are crucial for accurately forecasting the prepared T:M production cost. The estimated production cost for 100 mL of T:M is approximately $14.40, encompassing all expenses (e.g., Thymol, Menthol, electrical energy). The EcoScale synthesis score for T:M was calculated and compared with other published green solvents, such as ionic liquids and deep eutectic solvents (DES). As shown in Table 2, T:M achieved an impressive score of approximately 95%, positioning it on par with other natural DESs like choline chloride and betaine, as well as choline chloride-based and choline chloride/urea DESs. This result underscores T:M's synthesis as an exemplary green process according to EcoScale criteria. The development of natural deep

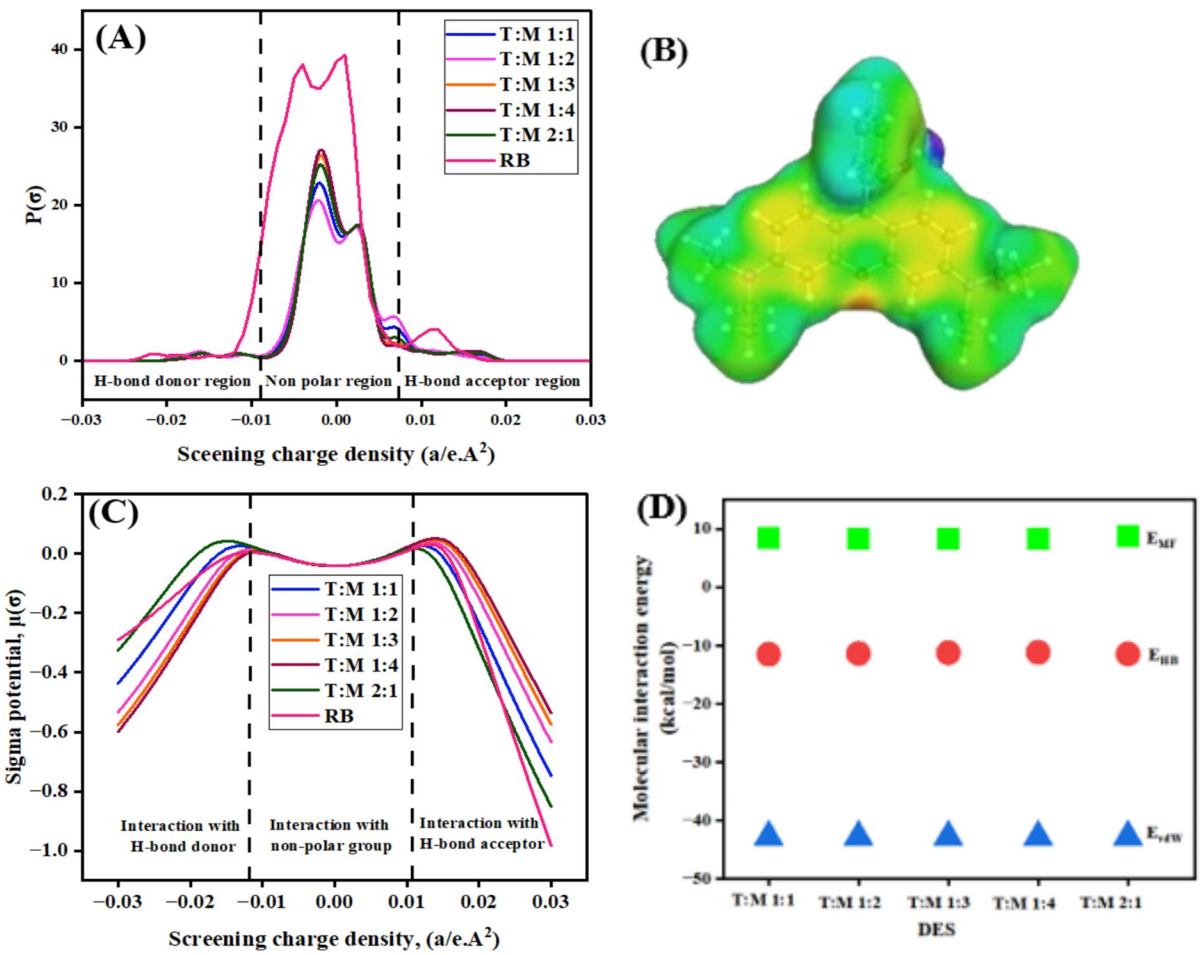



**Fig. 5** **A** σ-profile of T:M with RB, **B** σ-surface of RB, **C** σ-potential of T:M with RB, and **D** the $E_{vdW}$, $E_{HB,}$ and $E_{MF}$ of T:M at various molar ratios

**Table 2** Comparison of the EcoScale of the previous studies with T:M

| Solvent | EcoScale | | Reference |
|---|---|---|---|
| Benzyl imidazolium-based room temperature ionic liquids (RTILs) | Parameter | Penalty points (PPs) | Fan et al. (2021) |
| | Yield | 1 | |
| | Price of reaction components | 3 | |
| | Safety | 5 | |
| | Technical setup | 1 | |
| | Temperature/time | 3 | |
| | Workup and purification | 2 | |
| | Total PPs | 15 | |
| | Score | 85 | |
| 1-hexyl-2-phenyl-imidazolium bis(trifluoromethanesulfonyl)amide [HPhIm][$NTf_2$] | Parameter | Penalty points (PPs) | Kermanioryani et al. (2016) |
| | Yield | 1 | |
| | Price of reaction components | 3 | |
| | Safety | 5 | |
| | Technical setup | 1 | |
| | Temperature/time | 3 | |
| | Workup and purification | 2 | |
| | Total PPs | 15 | |
| | Score | 85 | |
| 1-benzyl-3-methyl-imidazolium bis(trifluoromethane sulfonyl)amide [BnMIm][$NTf_2$] | Parameter | Penalty points (PPs) | Kumar et al. (2020) |
| | Yield | 1 | |
| | Price of reaction components | 3 | |
| | Safety | 5 | |
| | Technical setup | 1 | |
| | Temperature/time | 3 | |
| | Workup and purification | 2 | |
| | Total PPs | 15 | |
| | Score | 85 | |
| 1-butyl-1-methypyrrolidinium bis(trifluoromethylsulfonyl)imide [bmpyrr][$Tf_2N$] | Parameter | Penalty points (PPs) | Lawal and Moodley (2015) |
| | Yield | 1 | |
| | Price of reaction components | 3 | |
| | Safety | 5 | |
| | Technical setup | 1 | |
| | Temperature/time | 3 | |
| | Workup and purification | 2 | |
| | Total PPs | 15 | |
| | Score | 85 | |
| 1-methyl,3-decahexyl imidazolium | Parameter | Penalty points (PPs) | Aroso et al. (2017) |
| | Yield | 1 | |
| | Price of reaction components | 3 | |
| | Safety | 5 | |
| | Technical setup | 1 | |
| | Temperature/time | 3 | |
| | Workup and purification | 2 | |
| | Total PPs | 15 | |
| | Score | 85 | |

**Table 2** (continued)

| Solvent | EcoScale | | Reference |
|---|---|---|---|
| Deep eutectic solvents from choline chloride and betaine | Parameter | Penalty points (PPs) | Alam et al. (2021) |
| | Yield | 0 | |
| | Price of reaction components | 0 | |
| | Safety | 5 | |
| | Technical setup | 0 | |
| | Temperature/time | 0 | |
| | Workup and purification | 0 | |
| | Total PPs | 5 | |
| | Score | 95 | |
| Choline chloride-based deep eutectic solvents | Parameter | Penalty points (PPs) | Sapir and Harries (2020) |
| | Yield | 0 | |
| | Price of reaction components | 0 | |
| | Safety | 5 | |
| | Technical setup | 0 | |
| | Temperature/time | 0 | |
| | Workup and purification | 0 | |
| | Total PPs | 5 | |
| | Score | 95 | |
| Choline Chloride/Urea | Parameter | Penalty points (PPs) | Omar and Sadeghi (2021) |
| | Yield | 0 | |
| | Price of reaction components | 0 | |
| | Safety | 5 | |
| | Technical setup | 0 | |
| | Temperature/time | 0 | |
| | Workup and purification | 0 | |
| | Total PPs | 5 | |
| | Score | 95 | |
| T:M | Parameter | Penalty points (PPs) | This study |
| | Yield | 0 | |
| | Price of reaction components | 0 | |
| | Safety | 5 | |
| | Technical setup | 0 | |
| | Temperature/time | 0 | |
| | Workup and purification | 0 | |
| | Total PPs | 5 | |
| | Score | 95 | |

eutectic solvents offers numerous advantages over ionic liquids, including cost-effectiveness, safety, eco-friendliness, simplicity, and ease of synthesis. This aligns with green chemistry principles by minimising the use and disposal of environmentally harmful organic reagents and promoting sustainability.

Moreover, the dye removal process is a crucial factor that reflects the economic viability and sustainability of the overall remediation approach. To demonstrate the economic efficiency and significant potential for environmental remediation of the studied DESs, the removal performance of a representative

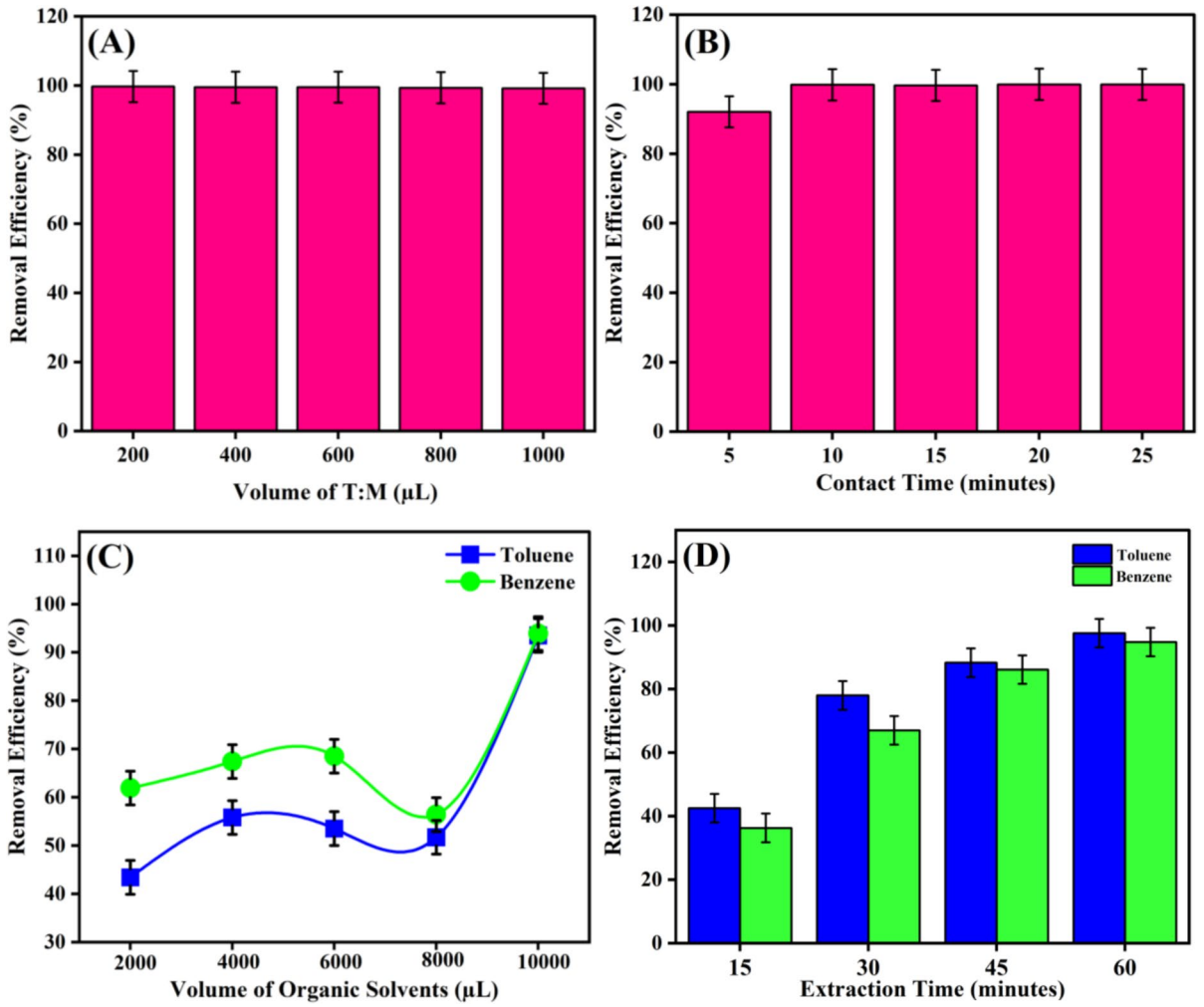



**Fig. 6** Effect of **A** volume of T:M, **B** contact time T:M, **C** volume of organic solvents, and **D** extraction time of organic solvents on the removal efficiency of RB

DES (T:M at a 1:1 molar ratio) was compared with that of conventional organic solvents (toluene and benzene). The comparison focused on extraction time and the volume of extractant required to achieve a high removal efficiency of RB. As depicted in Fig. 6 (A-D), the T:M 1:1 mixture exhibited exceptional dye removal efficiency, reaching 99% removal using only 400 µL of DES and just 10 min of extraction time. In contrast, toluene and benzene required 10,000 µL and 60 min to remove RB dye completely. This stark comparison highlights the superior performance of the proposed DES in dye remediation, achieving high removal efficiency with significantly lower extractant volume and reduced extraction time. These advantages underscore its potential to minimise waste and substantially reduce operational costs.

Furthermore, the dye removal performance of the studied DES (T:M 1:1) was further evaluated across a range of pH levels and against various dyes, including MB, CV, and SR. Remarkably, the results (Fig. 7(A-B)) revealed that the T:M 1:1 mixture maintained high removal efficiency for RB dye across all tested pH levels and demonstrated effective removal of the other dyes. This suggests that the DES holds strong potential as a versatile extractant for dye-contaminated wastewater, which typically contains a mixture of dye types and

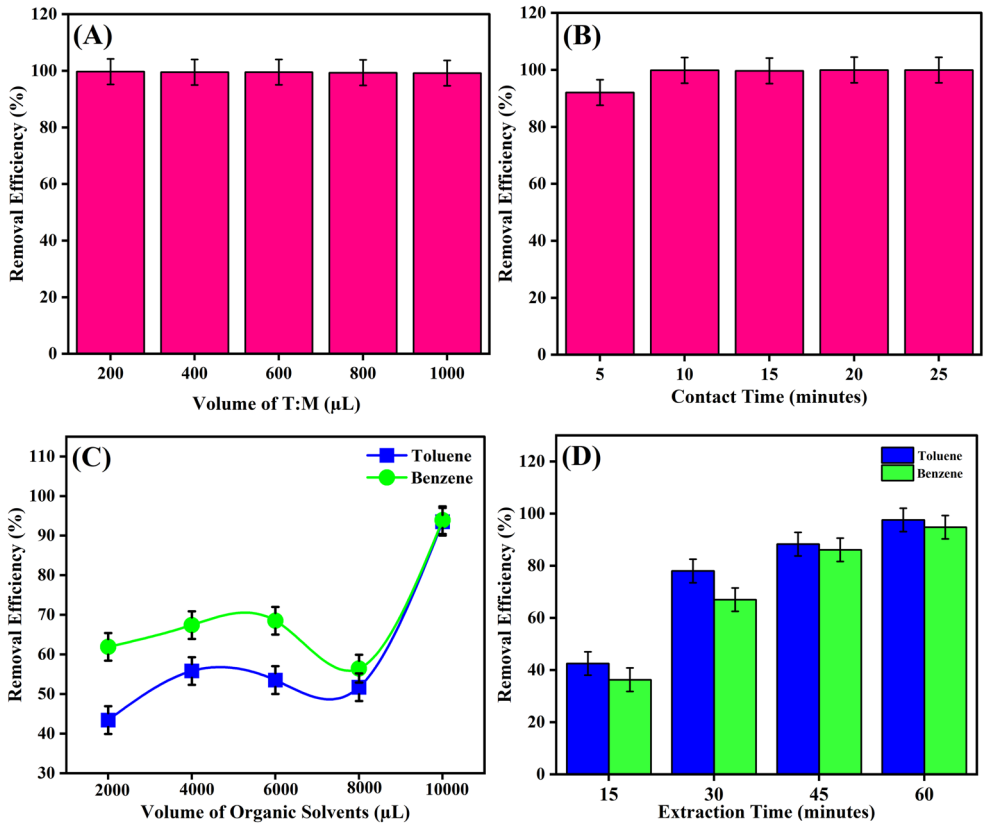



**Fig. 7** Effect of **A** pH of the solution on the removal efficiency of RB, **B** Removal efficiencies of DES toward various dyes, and **C** Phytotoxicity study of the studied DES (T:M 1:1) on pea (*Pisum sativum*) seeds

varies in pH. These findings confirm that the proposed DES is a promising, efficient, and sustainable solution for dye remediation. To evaluate the environmental impact of the proposed DES, its phytotoxicity was assessed using pea seeds (*Pisum sativum*) as a model system. Figure 7 (C) revealed that the percent seed germination remained unaffected at DES concentrations up to 0.1%, suggesting that low DES concentrations are non-toxic to pea seed germination. This finding is consistent with previous studies by Kang Zheng et al. (2025), and Yap and Gan 2024. An EcoScale score of 96 was assigned to the dye removal process, encompassing reagent use, instrumentation, occupational safety, and waste generation, highlighting its sustainability due to low operational costs, minimal waste production, and reduced energy usage.

### 3.6 Comparison of Dye Removal Performance of Proposed DES with Previous Published DES, Ionic Liquids (ILs), and Organic Solvents

This study presents the first application of T:M to remove Rhodamine B (RB) from aqueous solutions. The optimal remediation conditions and removal efficiency of the studied T:M were compared with those of other reported dye extractants. As shown in Table 3, the proposed DES demonstrated high removal efficiency for RB within a short period and using a minimal volume of extractant, suggesting that the proposed DES offers a simple and cost-effective method for dye removal, with advantages over other solvents reported for liquid–liquid extraction.

**Table 3** Comparison of the performance of present DESs with the reported DESs, Ionic liquids (ILs), and organic solvents for the remediation of dyes

| DESs | Extraction Method | Dye | Volume of DES (µL) | Contact time (min) | pH | Extraction efficiency (%) | Reference |
|---|---|---|---|---|---|---|---|
| T:M | Liquid–liquid extraction | Rhodamine B (RB) | 400 | 10 | 2–10 | 99 | This study |
| Tetrabutylammonium Bromide (TBAB:1-Nonanol)<br>Tetrabutylammonium Hydrogensulfate (TBAHS:1-Nonanol)<br>Tetrabutylammonium Iodide (TBAI:1-Nonanol) | Liquid–liquid extraction | Congo Red | 100000 | 30 | 7 | > 90 | Omar and Sadeghi (2021) |
| Tetrabutylammonium bromide: 1-octanol (TBAB: 1-octanol) | Liquid–liquid microextraction | Brilliant Blue FCF (E133) | 500 | 10 | 5 | > 95 | Rafati et al. (2025) |
| Thymol:acetanilide (Thy:ACN)<br>Thymol:acetamide (Thy:ACM) | Liquid–liquid extraction | Methylene blue (MB)<br>Rhodamine B (RB) | 1009.55 | 10 | - | > 80 | Olgun et al. (2024) |
| Choline chloride: Ethyl glycol<br>Choline chloride: 1,2-Butanediol<br>Choline chloride: glycerol<br>Choline chloride: 1,3-Butanediol<br>Choline chloride: 1,4-Butanediol | Ultrasonic-assisted extraction | Chrysoidine G (COG)<br>Astrazon orange G (AOG)<br>Astrazon orange R (AOR) | 1000 | 20 | - | > 60 | Zhu et al. (2017) |
| 1-octyl-3-methylimidazolium hexafluorophosphate ($[C_8MIM][PF_6]$) | Liquid–liquid microextraction | Malachite Green (MG)<br>Crystal Violet (CV) | 80 | 50 | 4 | > 91.7 | Zhang et al. (2012) |
| Tetrabutyl Ammonium Bromide | Liquid–liquid extraction | Brilliant orange 3R | 10,000 | 1080 | 2–12 | > 99 | Othman et al. (2010) |
| Toluene, kerosene, n-Dodecane, xylene, Dichloromethane, chloroform | Liqui-liquid extraction | Brilliant orange 3R | 10,000 | 1080 | - | 50–98 | Othman et al. (2010) |
| Trihexyltetradecylphosphonium decanoate | Liquid–liquid extraction | Reactive black, navy and royal | 10, 12.5, 50, 75, and 100 mg | 90 | 6–8 | > 80 | Dalari et al. (2022) |
| Benzene + Salicylic acid | Liquid–liquid extraction | Methylene Blue (MB) | 10,000 | 25 | 11 | 93 | Soniya and Muthuraman (2015) |

## 4 Conclusion

In this study, deep eutectic solvents (DESs) composed of Thymol and Menthol were synthesised for efficient organic dye removal through liquid–liquid extraction (LLE). Experimental results revealed that the proposed DES has an exceptional performance, removing 99% of Rhodamine B (RB) from aqueous solutions of 10 ppm under optimal conditions (400 µL of DES volume, 10 min of contact time, and pH 2–10). The proposed extractant effectively addresses limitations of conventional solvents in dye extraction processes, such as prolonged extraction durations, high volatility, expensive, complicated synthesis and large solvent volume requirements. EcoScale assessment demonstrated that the synthesis and dye removal processes employing the proposed DES are economically viable, operationally safe, and environmentally benign, characterised by minimal waste generation and low operator risk. Moreover, the solvent system showed broad applicability, achieving 70–98% removal efficiency for various textile dyes, including Methylene Blue (MB), Crystal Violet (CV) and Safranin (SR). Phytotoxicity assessment confirmed that studied T:M at low concentrations had no inhibitory effects on *Pisum sativum* (pea) seed germination, indicating its environmental compatibility for potential wastewater treatment applications. The findings of this study establish the developed method as an innovative approach for dye removal from aqueous systems, demonstrating significant potential as a sustainable alternative to conventional organic solvents in LLE process.

**Acknowledgements** The authors would like to acknowledge the research funding for research activities through the International Research Fund (INTERES) (9008-00056).

**Author Contributions** Ghee Kang Zheng: writing—review and editing, methodology, investigation, resources, data curation. Siti Khalijah Mahmad Rozi: writing—review and editing, methodology, investigation, resources, data curation. Ang Qian Yee: Interpretation of Computational result, supervision, and project administration. Rafizah Rahamathullah: Interpretation of modelling result, data curation, writing—review and editing. Saleha Shamsudin: conceptualization, methodology, formal analysis. Fairuz Liyana Mohd Rasdi: Interpretation of Computational result, investigation, writing—review and editing. Mohd Faisal Taha: writing—review and editing, visualization. Nidal M. Hussein; writing—review and editing, methodology. Faisal Aburub: writing—review and editing, visualization.

**Funding** Open access funding provided by The Ministry of Higher Education Malaysia and Universiti Malaysia Perlis.

**Data Availability** The manuscript has no associated data.

**Declarations**

**Competing interest** The authors declare that they have no known competing commercial interests or personal relationships that could have appeared to influence the work reported in this paper.

**Open Access** This article is licensed under a Creative Commons Attribution 4.0 International License, which permits use, sharing, adaptation, distribution and reproduction in any medium or format, as long as you give appropriate credit to the original author(s) and the source, provide a link to the Creative Commons licence, and indicate if changes were made. The images or other third party material in this article are included in the article's Creative Commons licence, unless indicated otherwise in a credit line to the material. If material is not included in the article's Creative Commons licence and your intended use is not permitted by statutory regulation or exceeds the permitted use, you will need to obtain permission directly from the copyright holder. To view a copy of this licence, visit http://creativecommons.org/licenses/by/4.0/.

## References

Adeyemi, I., Sulaiman, R., Almazroui, M., Al-Hammadi, A., & AlNashef, I. M. (2020). Removal of chlorophenols from aqueous media with hydrophobic deep eutectic solvents: Experimental study and COSMO RS evaluation. *Journal of Molecular Liquids, 311*, Article 113180.

Ahmed, H. L., Mohammed-Amin, S. M., & Fattahi, N. (2025). Speciation of As (III), As (V), organic arsenic and total arsenic in rice samples using natural deep eutectic solvent-based liquid phase microextraction followed by ETAAS. *International Journal of Environmental Analytical Chemistry*, 1–14.

Alam, M. A., Muhammad, G., Khan, M. N., Mofijur, M., Lv, Y., Xiong, W., & Xu, J. (2021). Choline chloride-based deep eutectic solvents as green extractants for the isolation of phenolic compounds from biomass. *Journal of Cleaner Production, 309*, Article 127445.

Al-Buriahi, A. K., Al-Gheethi, A. A., Kumar, P. S., Mohamed, R. M. S. R., Yusof, H., Alshalif, A. F., & Khalifa, N. A. (2022). Elimination of rhodamine B from textile wastewater using nanoparticle photocatalysts: A review for sustainable approaches. *Chemosphere, 287*, Article 132162.

Al-Gheethi, A. A., Azhar, Q. M., Kumar, P. S., Yusuf, A. A., Al-Buriahi, A. K., Mohamed, R. M. S. R., & Al-Shaibani, M. M. (2022). Sustainable approaches for removing Rhodamine B dye using agricultural waste adsorbents: A review. *Chemosphere, 287*, Article 132080.

Alqahtani, A. S. (2024). Indisputable roles of different ionic liquids, deep eutectic solvents and nanomaterials in green chemistry for sustainable organic synthesis. *Journal Of Molecular Liquids*. https://doi.org/10.1016/j.molliq.2024.124469

Amalina, F., Abd Razak, A. S., Krishnan, S., Zularisam, A. W., & Nasrullah, M. (2022). A review of eco-sustainable techniques for the removal of Rhodamine B dye utilizing biomass residue adsorbents. *Physics and Chemistry of the Earth, 128*, Article 103267.

Aroso, I. M., Paiva, A., Reis, R. L., & Duarte, A. R. C. (2017). Natural deep eutectic solvents from choline chloride and betaine–physicochemical properties. *Journal Of Molecular Liquids, 241*, 654–661.

Baginska, S., Golonko, A., Swislocka, R., & Lewandowski, W. (2023). Monoterpenes as medicinal agents: Exploring the pharmaceutical potential of p-cymene, p-cymenene, and γ-terpinene. *Acta Poloniae Pharmaceutica - Drug Research, 80*, 879–892.

Behbahani, M., Sobhi, H. R., & Esrafili, A. (2021). Combination of ultrasonic-assisted dispersive liquid phase microextraction with magnetic dispersive solid-phase extraction for the pre-concentration of trace amounts of atrazine in various water samples. *International Journal of Environmental Analytical Chemistry, 101*(5), 609–620.

Bouarab, A. F., Harvey, J. P., & Robelin, C. (2021). Viscosity models for ionic liquids and their mixtures. *Physical Chemistry Chemical Physics, 23*(2), 733–752.

Brijmohan, N., Moodley, K., & Narasigadu, C. (2021). Identification and screening of potential organic solvents for the liquid–liquid extraction of aromatics. *Organic Process Research & Development, 25*(10), 2230–2248.

Chabib, C. M., Ali, J. K., Abi Jaoude, M., Alhseinat, E., Adeyemi, I. A., & Al Nashef, I. M. (2022). Application of deep eutectic solvents in water treatment processes: A review. *Journal of Water Process Engineering, 47*, Article 102663.

Chen, Y., & Mu, T. (2021). Revisiting greenness of ionic liquids and deep eutectic solvents. *Green Chemical Engineering, 2*(2), 174–186.

Chen, Y., Zhang, F., Chang, Y., Wang, J., Zhang, Q., Yang, M., Liu, Z., & Zhang, Z. (2023a). Natural biomass soups (NBSs): New green solvents replacing ionic liquids and deep eutectic solvents for lithium-ion batteries recovery. *Energy & Fuels, 37*(23), 19076–19081.

Chen, L., Liao, S., Yu, D., Li, L., Mu, T., & Xue, Z. (2023b). Innovative aryl-based hydrophobic deep eutectic solvent for efficient removal of dyes and nanoplastics. *Separation and Purification Technology, 308*, Article 122903.

Chen, K., Dong, H., Ni, Z., Zhao, Y., Qian, Y., Wang, Y., & Xu, K. (2024). Selective extraction of anionic and cationic dyes using tailored hydrophobic deep eutectic solvents. *Talanta, 268*, Article 125312.

Cotroneo-Figueroa, V. P., Gajardo-Parra, N. F., López-Porfiri, P., Leiva, Á., Gonzalez-Miquel, M., Garrido, J. M., & Canales, R. I. (2022). Hydrogen bond donor and alcohol chain length effect on the physicochemical properties of choline chloride based deep eutectic solvents mixed with alcohols. *Journal of Molecular Liquids, 345*, Article 116986.

Dalari, B. L. S. K., Giroletti, C. L., Malaret, F. J., Skoronski, E., Hallett, J. P., Matias, W. G., Santos Klienchen Dalari, B. L., Lisboa Giroletti, C., Puerari, R. C., & Nagel-Hassemer, M. E. (2022). Application of a phosphonium-based ionic liquid for reactive textile dye removal: Extraction study and toxicological evaluation. *Journal of Environmental Management, 304*, Article 114322.

Duan, M., Luo, M., Yang, Z., Xiong, Y., Shi, P., Fang, S., & Qin, S. (2021). Application of choline-based deep eutectic solvent for the extraction of crude-oil contaminated soils. *Environmental Technology, 42*(18), 2896–2901.

El-Sayed, S. A., Khass, T. M., & Mostafa, M. E. (2024). Thermal degradation behaviour and chemical kinetic characteristics of biomass pyrolysis using TG/DTG/DTA techniques. *Biomass Conversion and Biorefinery, 14*(15), 17779–17803.

Fabre, E., & Murshed, S. S. (2021). A review of the thermophysical properties and potential of ionic liquids for thermal applications. *Journal of Materials Chemistry A, 9*(29), 15861–15879.

Fan, X. H., Wang, L. T., Chang, Y. H., An, J. Y., Zhu, Y. W., Yang, Q., & Fu, Y. J. (2021). Application of green and recyclable menthol-based hydrophobic deep eutectic solvents aqueous for the extraction of main taxanes from *Taxus chinensis* needles. *Journal of Molecular Liquids, 326*, Article 114970.

Freire, R. L., Sinzervinch, A., Marreto, R. N., & Kogawa, A. C. (2025). Excellent green analysis for quantification of gatifloxacin in eye drops by eco-scale assessment. *Revista Estudos-Revista de Ciências Ambientais e Saúde, 52,* 1–12.

Hansen, B. B., Spittle, S., Chen, B., Poe, D., Zhang, Y., Klein, J. M., Horton, A., Adhikari, L., Zelovich, T., Doherty, B. W., Gurkan, B., Maginn, E. J., Ragauskas, A., Dadmun, M., Zawodzinski, T. A., Baker, G. A., Tuckerman, M. E., Savinell, R. F., & Sangoro, J. R. (2020). Deep eutectic solvents: A review of fundamentals and applications. *Chemical Reviews, 121*(3), 1232–1285.

Hussin, S. A. M., Varanusupakul, P., Shahabuddin, S., Hui, B. Y., & Mohamad, S. (2020). Synthesis and characterization of green menthol-based low transition temperature mixture with tunable thermophysical properties as hydrophobic low viscosity solvent. *Journal of Molecular Liquids, 308*, Article 113015.

Hussin, S. A. M., Varanusupakul, P., Kassim, M. A., Rozi, S. K. M., & Mohamad, S. (2021). Vortex assisted dispersive liquid–liquid microextraction based on low transition temperature mixture solvent for the HPLC determination of pyrethroids in water samples: Experimental study and COSMO-RS. *Microchemical Journal, 171*, Article 106780.

Ijardar, S. P., Singh, V., & Gardas, R. L. (2022). Revisiting the physicochemical properties and applications of deep eutectic solvents. *Molecules, 27*(4), 1368.

Jiang, G., He, K., Chen, M., Yang, L., Yang, Y., Tang, T., & Tian, Y. (2025). Improvement of mechanical and bioactive properties of chitosan films plasticized with novel thymol-based deep eutectic solvents. *Food Hydrocolloids, 158*, Article 110480.

Jin, J. C., Shen, N. N., Wang, Z. P., Peng, Y. C., & Huang, X. Y. (2021). Photoluminescent ionic metal halides based on s2 typed ions and aprotic ionic liquid cations. *Coordination Chemistry Reviews, 448*, Article 214185.

Kang Zheng, G., Rozi, S. K. M., Mat Hussin, S. A., Ang, Q. Y., Rahamathullah, R., Tan Tiek Aun, A., & Taha, M. F. (2025). New thymol and phenol-based deep eutectic solvents for effective remediation of dyes: experimental and theoretical investigations. *The Journal of The Textile Institute*, 1–17.

Kermanioryani, M., Mutalib, M. A., Gonfa, G., El-Harbawi, M., Mazlan, F. A., Lethesh, K. C., & Leveque, J. M. (2016). Using tunability of ionic liquids to remove methylene blue from aqueous solution. *Journal of Environmental Chemical Engineering, 4*(2), 2327–2332.

Khan, A. S., Ibrahim, T. H., Rashid, Z., Khamis, M. I., Nancarrow, P., & Jabbar, N. A. (2021). COSMO-RS based screening of ionic liquids for extraction of phenolic compounds from aqueous media. *Journal of Molecular Liquids, 328*, Article 115387.

Khan, H. W., Khan, M. K., Moniruzzaman, M., Al Mesfer, M. K., Danish, M., Irshad, K., & Chelliapan, S. (2023). Evaluating ionic liquids for its potential as eco-friendly solvents for naproxen removal from water sources using COSMO-RS: Computational and experimental validation. *Environmental Research, 231*, Article 116058.

Khatibi, S. A., Hamidi, S., & Siahi-Shadbad, M. R. (2022). Application of liquid-liquid extraction for the determination of antibiotics in the foodstuff: Recent trends and developments. *Critical Reviews in Analytical Chemistry, 52*(2), 327–342.

Kianfar, E., & Mafi, S. (2021). Ionic liquids: Properties, application, and synthesis. *Fine Chemical Engineering, 2*(1), 21–29.

Krause, S. T., Liao, P., Crocoll, C., Boachon, B., Förster, C., Leidecker, F., & Degenhardt, J. (2021). The biosynthesis of thymol, carvacrol, and thymohydroquinone in Lamiaceae proceeds via cytochrome P450s and a short-chain dehydrogenase. *Proceedings of the National Academy of Sciences, 118*(52), Article e2110092118.

Kumar, V., Singh, M., Behera, K., & Pandey, S. (2020). Ionic liquid induced removal of Rhodamine B from water. *Journal of Molecular Liquids, 319*, Article 114195.

Lamarca, R. S., Ferreira, S. D. S., Paganini, É. R., Ferreira, N. D. S., Ayala-Durán, S. C., Isquibola, G., & Gonzalez, M. H. (2024). Sustainable cadmium extraction from sewage sludge samples: A novel approach with hydrophobic deep eutectic solvents and ultrasound-assisted extraction (HDES-UAE) prior to ICP-MS analysis. *Journal of Molecular Liquids, 398*, Article 124264.

Lawal, I. A., & Moodley, B. (2015). Synthesis, characterisation and application of imidazolium based ionic liquid modified montmorillonite sorbents for the removal of amaranth dye. *RSC Advances, 5*(76), 61913–61924.

Malolan, R., Gopinath, K. P., Vo, D. V. N., Jayaraman, R. S., Adithya, S., Ajay, P. S., & Arun, J. (2021). Green ionic liquids and deep eutectic solvents for desulphurization, denitrification, biomass, biodiesel, bioethanol and hydrogen fuels: A review. *Environmental Chemistry Letters, 19*, 1001–1023.

Marchel, M., Cieśliński, H., & Boczkaj, G. (2022). Thermal instability of choline chloride-based deep eutectic solvents and its influence on their toxicity— Important limitations of DESs as sustainable materials. *Industrial & Engineering Chemistry Research, 61*(30), 11288–11300.

Martínez, G. M., Townley, G. G., & Martínez-Espinosa, R. M. (2022). Controversy on the toxic nature of deep eutectic solvents and their potential contribution to environmental pollution. *Heliyon*. https://doi.org/10.1016/j.heliyon.2022.e12567

Mejías, C., Arenas, M., Martín, J., Santos, J. L., Aparicio, I., & Alonso, E. (2025). Green assessment of analytical procedures for the determination of pharmaceuticals in sewage sludge and soil. *Critical Reviews in Analytical Chemistry, 55*(2), 278–291.

Mero, A., Koutsoumpos, S., Giannios, P., Stavrakas, I., Moutzouris, K., Mezzetta, A., & Guazzelli, L. (2023). Comparison of physicochemical and thermal properties of choline chloride and betaine-based deep eutectic solvents: The influence of hydrogen bond acceptor and hydrogen bond donor nature and their molar ratios. *Journal of Molecular Liquids, 377*, Article 121563.

Mydeen, K. M., Kanth, J. P., Hariharan, A., Balaji, K., Rameshkumar, S., Rathika, G., & Alagar, M. (2022). Fully bio-based polybenzoxazines derived from thymol: Thermal stability, hydrophobicity and corrosion resistant properties. *Journal of Polymers and the Environment, 30*(12), 5301–5312.

Nahar, Y., & Thickett, S. C. (2021). Greener, faster, stronger: The benefits of deep eutectic solvents in polymer and materials science. *Polymers, 13*(3), 447.

Nam, N. N., Do, H. D. K., Trinh, K. T. L., & Lee, N. Y. (2023). Design strategy and application of deep eutectic solvents for green synthesis of nanomaterials. *Nanomaterials, 13*(7), Article 1164.

Nguyen, D., Van Huynh, T., Nguyen, V. S., Cao, P. L. D., Nguyen, H. T., Wei, T. C., & Nguyen, P. T. (2021). Choline chloride-based deep eutectic solvents as effective electrolytes for dye-sensitized solar cells. *RSC Advances, 11*(35), 21560–21566.

Olgun, M., Özak, S. S., & Dalmaz, A. (2024). Spectrophotometric determination for green hydrophobic deep eutectic solvent-based microextraction of Brilliant Blue FCF (E133) from beverages. *Journal of Chromatography A, 1736*, Article 465374.

Omar, K. A., & Sadeghi, R. (2021). Novel nonanol-based deep eutectic solvents: Thermophysical properties and their applications in liquid-liquid extraction and amino acid detection. *Journal of Molecular Liquids, 336*, Article 116359.

Oshima, T., & Ito, M. (2021). Sedative effects of l-menthol, d-camphor, phenylethyl alcohol, and geraniol. *Journal of Natural Medicines, 75*, 319–325.

Othman, N., Mili, N., Zailani, S. N., & Mohammad, N. A. B. (2010). Extraction of remazol brilliant orange 3R from textile wastewater using tetrabutyl ammonium bromide. *Jurnal Teknologi (Sciences & Engineering)*, 29–39.

Panić, M., Cvjetko Bubalo, M., & Radojčić Redovniković, I. (2021). Designing a biocatalytic process involving deep eutectic solvents. *Journal of Chemical Technology & Biotechnology, 96*(1), 14–30.

Peng, D., & Minceva, M. (2024). Predicting the density and viscosity of deep eutectic solvents at atmospheric and elevated pressures. *Fluid Phase Equilibria, 582*, Article 114086.

Qi, D., Cao, Z., Tu, Y., Liu, K., Gao, F., Zhou, Z., Du, C., & Ren, Z. (2025). Bio-derived thymol/MEA deep eutectic solvent for efficient CO2 absorption. *Separation and Purification Technology*. https://doi.org/10.1016/j.seppur.2025.133569

Quaid, T., & Reza, T. (2023). COSMO-RS predictive screening of type 5 hydrophobic deep eutectic solvents for selective platform chemicals absorption. *Journal of Molecular Liquids, 382*, Article 121918.

Rafati, S., Ebrahimi, N., & Sadeghi, R. (2025). New family of type V natural hydrophobic deep eutectic solvents based on thymol-acetamide/acetanilide: Characteristics, intermolecular interactions and applications in liquid–liquid extraction. *Separation and Purification Technology, 359*, Article 130583.

Rahman, M. H., Khajeh, A., Panwar, P., Patel, M., Martini, A., & Menezes, P. L. (2022). Recent progress on phosphonium-based room temperature ionic liquids: Synthesis, properties, tribological performances and applications. *Tribology International, 167*, Article 107331.

Rahman, M. A., Ndiaye, M., Weclawski, B., & Farrell, P. (2025). Palmyra palm shell (*Borassus flabellifer*) properties part 3: Insights into its morphological, chemical, and thermal properties after alkali treatment. *Engineering Reports, 7*(4), Article e70103.

Rashid, S. N., Hizaddin, H. F., Hayyan, A., Hasikin, K., Razak, S. A., Mokhtar, M. I., & Azizan, M. M. (2022). Deep eutectic solvents for the removal of lead contaminants in mangrove soil. *Journal of Environmental Chemical Engineering, 10*(2), Article 107264.

Saigl, Z. M. (2021). Various adsorbents for removal of rhodamine B dye: A review. *Indonesian Journal of Chemistry, 21*(4), 1039–1056.

Sapir, L., & Harries, D. (2020). Restructuring a deep eutectic solvent by water: The nanostructure of hydrated choline chloride/urea. *Journal of Chemical Theory and Computation, 16*(5), 3335–3342.

Sekharan, T. R., Chandira, R. M., Tamilvanan, S., Rajesh, S. C., & Venkateswarlu, B. S. (2022). Deep eutectic solvents

as an alternate to other harmful solvents. *Biointerface Research In Applied Chemistry, 12*(1), 847–860.

Sereshti, H., Abdolhosseini, G., Soltani, S., Jamshidi, F., & Nouri, N. (2021). Natural thymol-based ternary deep eutectic solvents: Application in air-bubble assisted-dispersive liquid-liquid microextraction for the analysis of tetracyclines in water. *Journal of Separation Science, 44*(19), 3626–3635.

Sharifi, N., Abdollahi, A., Zarenezhad, E., Fereydouni, N., Rahmani, M., & Osanloo, M. (2025). Poly caprolactone nanofibers containing camphor and thymol: Fabrication, characterization, and antimicrobial applications. *BioNano-Science, 15*(1), 1–11.

Singh, S. K., & Savoy, A. W. (2020). Ionic liquids synthesis and applications: An overview. *Journal of Molecular Liquids, 297*, Article 112038.

Soniya, M., & Muthuraman, G. (2015). Recovery of methylene blue from aqueous solution by liquid–liquid extraction. *Desalination and Water Treatment, 53*(9), 2501–2509.

Thakur, A., & Kaur, H. (2017). Response surface optimization of Rhodamine B dye removal using paper industry waste as adsorbent. *International Journal of Industrial Chemistry, 8*, 175–186.

Tian, S., Wang, X., Wang, C., Li, L., & Wei, W. (2023). Highly sensitive and label-free electrochemical sensor for menthol detection. *Journal of Electroanalytical Chemistry, 941*, Article 117540.

Tiwari, R. C., Dikshit, M., Mittal, B., & Sharma, V. B. (2022). Effects of water pollution-A review article. *Journal of Ayurveda and Integrated Medical Sciences, 7*(5), 63–68.

Uğan, M., Onac, C., Kaya, A., Köseoğlu, D., & Akdoğan, A. (2024). Removal of reactive red 195 dye from textile industry wastewater with deep eutectic solvent-based green extraction. *Journal of Molecular Liquids, 398*, Article 124249.

Velez, C., & Acevedo, O. (2022). Simulation of deep eutectic solvents: Progress to promises. *Wiley Interdisciplinary Reviews: Computational Molecular Science, 12*(4), Article e1598.

Wang, Z., Zhang, F., Sun, Y., Zheng, L., Shen, Y., Fu, D., Li, W., Pan, A., Wang, L., Xu, J., Hu, J., & Wu, X. (2021). Intrinsically nonflammable ionic liquid-based localized highly concentrated electrolytes enable high-performance Li-metal batteries. *Advanced Energy Materials, 11*(17), Article 2003752.

Yap, P. G., & Gan, C. Y. (2024). Exploration of potential application of low phytotoxic alkaline deep eutectic solvent (DES) in protein extraction and bioactive applications. *Journal of Molecular Liquids, 409*, Article 125521.

Yu, D., Xue, Z., & Mu, T. (2021). Eutectics: Formation, properties, and applications. *Chemical Society Reviews, 50*(15), 8596–8638.

Zhang, Z., Zhou, K., Bu, Y. Q., Shan, Z. J., Liu, J. F., Wu, X. Y., Yang, L.-Q., & Chen, Z. L. (2012). Determination of malachite green and crystal violet in environmental water using temperature-controlled ionic liquid dispersive liquid–liquid microextraction coupled with high performance liquid chromatography. *Analytical Methods, 4*(2), 429–433.

Zhang, T., Zheng, S., You, S., Huang, D., & Cheng, Y. X. (2022). Design and synthesis of potential fungicidal compounds derived from natural products,(-)-menthol and (-)-borneol. *Medicinal Chemistry Research, 31*(2), 307–315.

Zhang, W. X., Gao, Y. R., Xue, R., Nguyen, W., Chen, W., Wang, J. H., & Shu, Y. (2023). Liquid formulations based on ionic liquids in biomedicine. *Materials Today Physics, 30*, Article 100925.

Zhao, Y., Han, B., & Liu, Z. (2021). Ionic-liquid-catalyzed approaches under metal-free conditions. *Accounts of Chemical Research, 54*(16), 3172–3190.

Zhao, J., Wang, M., Lee, J., Ali, Z., & Khan, I. A. (2025). Characterization, differentiation, and adulteration detection of peppermint essential oil: An NMR approach. *Journal of Pharmaceutical and Biomedical Analysis*. https://doi.org/10.1016/j.jpba.2025.116941

Zheng, B., Yuan, Y., Xiang, J., Jin, W., Johnson, J. B., Li, Z., Wang, C., & Luo, D. (2022). Green extraction of phenolic compounds from foxtail millet bran by ultrasonic-assisted deep eutectic solvent extraction: Optimization, comparison and bioactivities. *LWT - Food Science and Technology, 154*, Article 112740.

Zheng, G. K., Rozi, S. K. M., Ang, Q. Y., Rahamathullah, R., Yaakub, A. R. W., Anuar, A., Rasdi. F. L. M., Taha, M. F., Hussein, N. M., Aburub, F., & Hussin, S. A. M. (2025). Hydrophobic deep eutectic solvent with antibacterial activity for remediation of crystal violet dye: Experimental and theoretical investigations. *International Journal of Environmental Science and Technology*, *22*, 13731–13747.

Zhu, S., Liu, D., Zhu, X., Su, A., & Zhang, H. (2017). Extraction of illegal dyes from red chili peppers with choliniumbased deep eutectic solvents. *Journal of Analytical Methods in Chemistry, 2017*(1), Article 2753752.

Zhu, N., Zhang, K., Wu, F., Bai, Y., & Wu, C. (2021). Ionic liquid-based electrolytes for aluminum/magnesium/sodium-ion batteries. *Energy Material Advances*. https://doi.org/10.34133/2021/9204217

**Publisher's Note** Springer Nature remains neutral with regard to jurisdictional claims in published maps and institutional affiliations.